

SYNTHESIS, STRUCTURE, PHOTOLUMINESCENCE AND THEORETICAL STUDY OF A NOVEL PYRAZINE COMPLEX

Xiu-Guang YI,^{a,b} Jian-Gen HUANG,^a Wen-Tong CHEN,^{a,c,d,*} Yin-Feng WANG^a and Jian-Ping ZOU^c

^aInstitute of Applied Chemistry, Jiangxi Province Key Laboratory of Coordination Chemistry, School of Chemistry and Chemical Engineering, Jinggangshan University, Ji'an, Jiangxi 343009, China

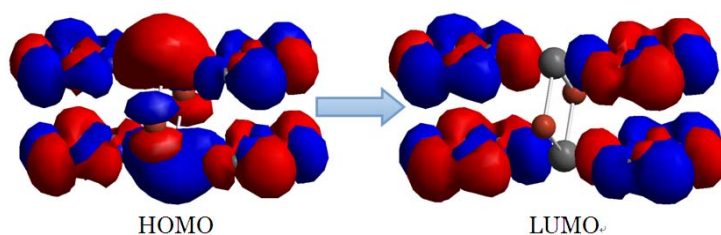
^bSchool of Materials Science and Engineering, Nanchang University, Nanchang, Jiangxi 330000, China

^cKey Laboratory of Jiangxi Province for Persistent Pollutants Control and Resources Recycle (Nanchang Hangkong University), Nanchang, Jiangxi 330000, China

^dState Key Laboratory of Structural Chemistry, Fujian Institute of Research on the Structure of Matter, Chinese Academy of Sciences, Fuzhou, Fujian 350002, China

Received June 22, 2017

A novel pyrazine complex, namely, $[\text{CdBr}_2(\text{C}_4\text{H}_4\text{N}_2)]_n$ (**1**, $\text{C}_4\text{H}_4\text{N}_2$ = pyrazine), has been synthesized through solvothermal reactions and structurally characterized by single-crystal X-ray diffraction. Compound **1** crystallizes in the space group $C222$ of the orthorhombic system with two formula units in a cell: $a = 7.566(3)$, $b = 12.554(6)$, $c = 3.8888(14)$ Å, $V = 369.4(3)$ Å³, $\text{C}_4\text{H}_2\text{Br}_2\text{CdN}_2$, $M_r = 350.30$ g/mol, $D_c = 3.150$ g/cm³, $S = 1.030$, $\mu(\text{MoK}\alpha) = 13.681$ mm⁻¹, $F(000) = 316$, $R = 0.0356$, $wR = 0.1018$. The cadmium ion is surrounded by four bromide ions and two nitrogen atoms from two pyrazine ligands, yielding a slightly distorted octahedron. The neighboring cadmium ions interconnect together via two bromide ions to form an infinite chain running along the c direction. The chains then link together by the pyrazine ligands to construct a two-dimensional (2-D) layer running parallel to the ac plane. Complex **1** displays an emission in the green region. Theoretical study discovers that the emission is originated from the metal-to-ligand charge-transfer (MLCT) and the ligand-to-ligand charge-transfer (LLCT) transition.



INTRODUCTION

In recent years, the crystal engineering of the inorganic-organic hybrid complexes has attracted more and more interest due to their potential applications in the areas of zeolite-like materials, gas adsorption materials, magnetic materials, catalysts, photoluminescence materials, and so on.¹⁻⁵ Moreover, the aesthetic perspective is another important reason. Regarding to the large number of inorganic-organic hybrid complexes, their charming structures that can be designed and prepared by self-assembling metal centres and various ligands attract

lots of scientists. Up to date, the design and synthesis of transition metal-containing inorganic-organic hybrid complexes have become widespread.⁶⁻¹⁰ To our knowledge, amongst the transition metal-containing inorganic-organic hybrid complexes, IIB (group 12, *i.e.* Zn, Cd, Hg) metal-containing inorganic-organic hybrid complexes are especially attractive because they can be potentially used in the fields such as photoluminescent materials, photoelectric materials, nonlinear optics materials, semiconductors, and so forth.¹¹⁻¹⁴

N-donor ligands are useful building blocks to construct inorganic-organic hybrid complexes due

* Corresponding author: wtchen@jgsu.edu.cn

to their ability of coordinating to metal ions by means of their nitrogen atoms. As one of the N-donor ligands, pyrazine is a very interesting unit in building inorganic-organic hybrid complexes with an extended structure because it has two nitrogen atoms in the contrapositions, which allows it to coordinate to two metal ions as a bridge. Therefore, pyrazine has been broadly applied to synthesize novel inorganic-organic hybrid complexes and a lot of pyrazine inorganic-organic hybrid complexes have thus far been documented.¹⁵⁻¹⁸

As a result, we recently become interested in the crystal engineering of IIB-based inorganic-organic hybrid complexes with pyrazine as a ligand. In this work, we report the synthesis, crystal structure, photoluminescence and time-dependent density functional theory (TDDFT) calculation of a novel pyrazine complex $[\text{CdBr}_2(\text{C}_4\text{H}_4\text{N}_2)]_n$ (**1**, $\text{C}_4\text{H}_4\text{N}_2 =$ pyrazine) which was prepared from a solvothermal reaction. This complex is characteristic of a two-dimensional layered structure.

EXPERIMENTAL

All reactants and chemicals are AR grade, obtained commercially and used without further purification. FT-IR spectra were recorded with a KBr pellet in the region of 400–4000 cm^{-1} on a PerkinElmer Spectrum-One spectrometer. The photoluminescent measurements were performed at room temperature in the solid-state on a computer-controlled JY FluoroMax-3 spectrometer. TDDFT calculation based on the

X-ray structure was carried out with Gaussian03 suite of programs. The electron density figures of the molecular orbitals were obtained with ChemOffice Ultra 7.0 graphics program.

Synthesis of $[\text{CdBr}_2(\text{C}_4\text{H}_4\text{N}_2)]_n$ (1**):** A mixture containing $\text{CdBr}_2 \cdot 4\text{H}_2\text{O}$ (1 mmol, 344 mg), 2-pyrazinecarboxylic acid (1 mmol, 124 mg) and 10 mL ethanol was loaded in a 25 mL Teflon-lined stainless steel vessel, which was heated at 180 °C for one week and then cooled down to room temperature at 6 °C/h. Colorless block crystals suitable for X-ray analysis were collected, separated, washed with distilled water, and then dried in air. The yield was 43% (based on cadmium). FT-IR peaks (KBr, cm^{-1}): 3442(vs), 3226(s), 2147(w), 1630(m), 1551(w), 1419(s), 1118(vs), 1049(s), 995(w), 891(m), 788(m), 655(w), 621(m), 591(w), 517(w), 448(m).

X-ray structure determination: The reflection data were collected on a Rigaku Mercury CCD X-ray diffractometer equipped with graphite monochromated Mo- $K\alpha$ radiation ($\lambda = 0.71073 \text{ \AA}$) with the use of ω scan technique. CrystalClear software was applied for the data reduction and the empirical absorption corrections. The structure was solved by the direct method with SHELXS-97 and refined by full-matrix least-squares method with SHELXL-97 program package. The successive difference Fourier maps based on these atomic positions generated all of the non-hydrogen atoms, which were refined anisotropically. The hydrogen atoms were yielded on idealized positions. A summary of crystallographic data and structural analyses is given in Table 1, and selected bond distances and bond angles from X-ray structure analysis are shown in Table 2. Crystallographic data for the structural analysis have been deposited with the Cambridge Crystallographic Data Centre, CCDC No. 1495546. Copies of this information may be obtained free of charge from the Director, CCDC, 12 Union Road, Cambridge, CBZ 1EZ, UK (Fax: +44-1223-336033; email: deposit@ccdc.cam.ac.uk or www:http://www.ccdc.cam.ac.uk).

Table 1

Summary of Crystallographic Data and Structure Analysis for **1**

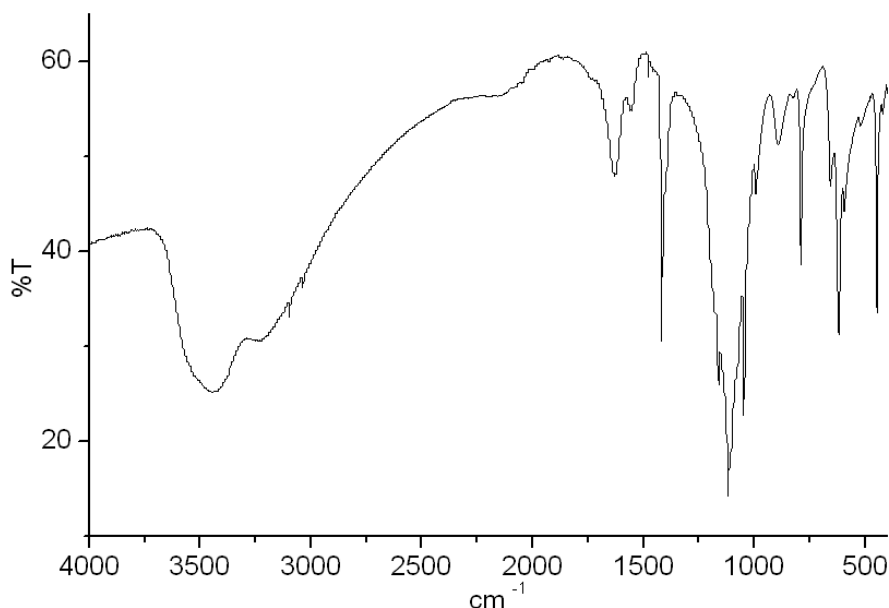
Empirical formula	$\text{C}_4\text{H}_2\text{Br}_2\text{CdN}_2$
Color and habit	colorless block
Crystal size (mm)	0.15 0.12 0.08
Crystal system	Orthorhombic
Space group	C222
a (Å)	7.566(3)
b (Å)	12.554(6)
c (Å)	3.8888(14)
β (°)	90
V (Å ³)	369.4(3)
Formula weight	350.30
Z	2
Theta range (°)	3.14 – 24.98
Reflections collected	1083
Independent, observed reflections (R_{int})	331, 320 (0.0702)
Density(cal.) (g/cm^3)	3.150
Absorption coefficient (mm^{-1})	13.681
Temperature(K)	296(2)
$F(000)$	316
$R1, wR2$	0.0356, 0.1018
Goodness-of-fit	1.030
Largest and Mean Delta/Sigma	0.001, 0
$\Delta\rho$ (max, min) ($\text{e}/\text{\AA}^3$)	1.027, -1.144

Table 2

Selected Bond Lengths (Å) and Bond Angles (°) of **1**

Cd(1)-N(1)	2.397(3)	N(1)#1-Cd(1)-Br(1)#2	90.0
Cd(1)-N(1)#1	2.397(3)	N(1)-Cd(1)-Br(1)#3	90.0
Cd(1)-Br(1)	2.7494(9)	N(1)#1-Cd(1)-Br(1)#3	90.0
Cd(1)-Br(1)#1	2.7494(9)	N(1)-Cd(1)-Br(1)#1	90.0
Cd(1)-Br(1)#2	2.7494(9)	N(1)#1-Cd(1)-Br(1)#1	90.0
Cd(1)-Br(1)#3	2.7494(9)	Br(1)-Cd(1)-Br(1)#3	90.02(4)
N(1)-Cd(1)-N(1)#1	180.0	Br(1)#2-Cd(1)-Br(1)#3	89.98(4)
N(1)-Cd(1)-Br(1)	90.0	Br(1)-Cd(1)-Br(1)#2	180.000(11)
N(1)#1-Cd(1)-Br(1)	90.0	Br(1)-Cd(1)-Br(1)#1	89.98(4)
N(1)-Cd(1)-Br(1)#2	90.0	Br(1)#2-Cd(1)-Br(1)#1	90.02(4)

Symmetry codes: #1 $-x+1, -y, z$; #2 $-x+1, -y, z+1$; #3 $x, y, z+1$; #4 $x, y, z-1$; #5 $x, -y, -z$; #6 $-x, y, -z$.

Fig. 1 – FT-IR spectra of **1**.

RESULTS AND DISCUSSION

FT-IR Spectrum

The starting material is 2-pyrazinecarboxylic acid, but pyrazine is found in the title complex. This suggests that an in situ reaction has occurred during the solvothermal process. As for the title complex, its FT-IR bands are mainly existed in the frequency range of 500 — 1500 cm^{-1} , as shown in Fig. 1. The very strong vibration at 3442 cm^{-1} can be ascribed to the characteristic peak of OH vibration of water molecules. The strong vibration locating at 3226 cm^{-1} corresponds to the C-H bending vibration of the pyrazine group. The intensive vibration residing at 1419 cm^{-1} can be assigned to the stretching vibration of the pyrazine ring. The FT-IR bands existed in the frequency range of 788—1049 cm^{-1} can be assigned to the bending vibrations of the pyrazine ring. The

vibration bands locating at 655 cm^{-1} , 591 cm^{-1} , 517 cm^{-1} and 448 cm^{-1} can be ascribed to the stretching vibration of Cd-Br bonds.

Crystal Structure

The crystal structure of complex **1** was found by the single-crystal X-ray diffraction method. Regarding to complex **1**, its ORTEP drawing with 20% thermal ellipsoids is presented in Fig. 2. The single-crystal X-ray diffraction analysis revealed that its molecular structure is belonged to the $C222$ space group of the orthorhombic system with two unit formula, *i.e.* $[\text{CdBr}_2(\text{C}_4\text{H}_4\text{N}_2)]$ in one cell. All the crystallographic independent atoms of **1** are in special positions, except for the C1 atom. The asymmetric unit consists of a quarter of cadmium ion, half of bromide ion, and a quarter of pyrazine ligand. The molecular structure of **1** is composed of a neutral two-dimensional (2-D)

$[\text{CdBr}_2(\text{C}_4\text{H}_4\text{N}_2)]_n$ layer. The cadmium ion is surrounded by four bromide ions and two nitrogen atoms from two pyrazine ligands, forming a slightly distorted octahedron. The neighboring cadmium ions interconnect together via two bromide ions to form an infinite chain running along the c direction. The chains then link together by the pyrazine ligands to construct a 2-D layer running parallel to the ac plane, as shown in Fig. 3. These layers then stack together via the van der Waals interactions to complete the crystal packing structure (Fig. 4). The bond lengths of Cd-Br and Cd-N are 2.7494(9) Å and 2.397(3) Å, respectively, which are comparable with those found in the literature.¹⁹⁻²⁵ The bond angles of $\angle \text{N-Cd-N}$ and $\angle \text{N-Cd-Br}$ are 180° and 90° , respectively. The bond angles of $\angle \text{Br-Cd-Br}$ are 90° and 180° . The result of the bond valence calculation discovered that the cadmium ion is in a +2 oxidation state (Cd1: 2.03).

Fluorescence Spectrum

Taking into account the potential photoluminescence property of the cadmium ion and pyrazine ligand, the solid-state photoluminescence measurements of complex **1** was conducted at room temperature and the result is given in Fig. 5. The photoluminescence excitation spectrum of complex **1** shows that the effective energy absorption is dominantly occurred in the wavelength region of 300–400 nm. The excitation band of complex **1** under the emission of 560 nm has a maximum band at 368 nm. Furthermore, we also carried out the corresponding photoluminescence emission spectrum with the use of the excitation wavelength of 368 nm for complex **1**, and the result is also shown in Fig. 5. We found that the photoluminescence emission spectrum exhibits a wide and intense emission band in the green region with a maximum value of 560 nm.

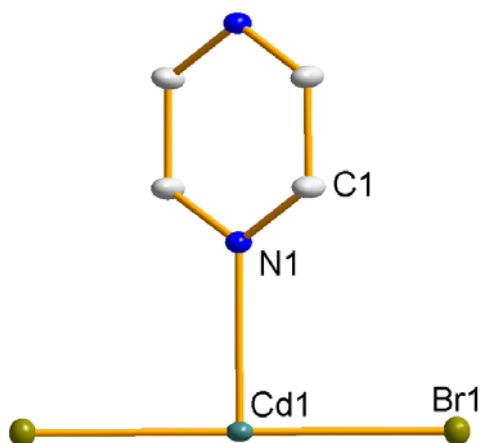


Fig. 2 – ORTEP drawing of **1** with 20% thermal ellipsoids. Hydrogen atoms are omitted for clarity.

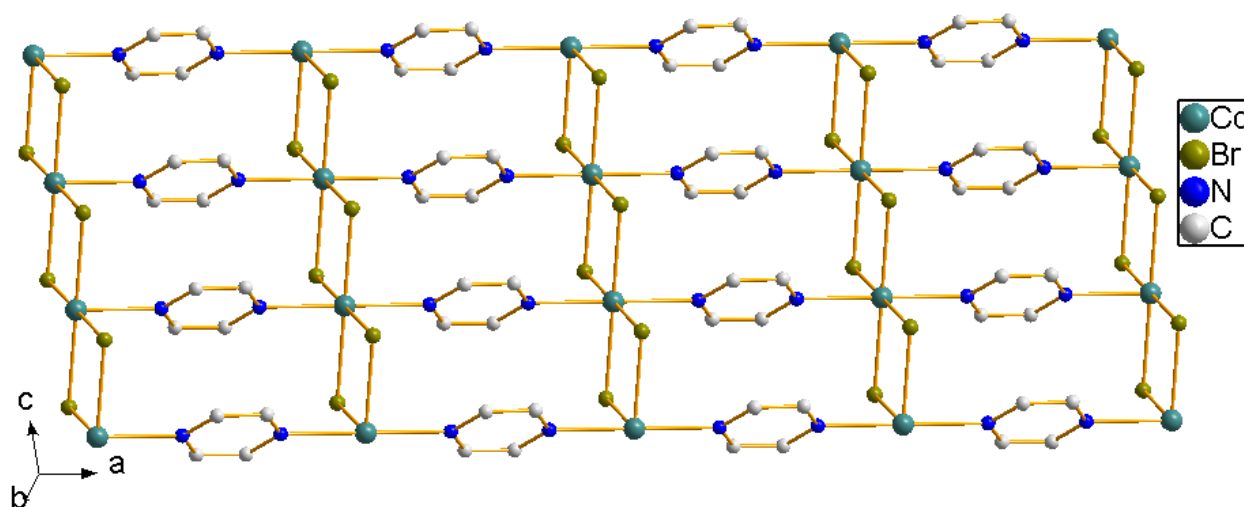


Fig. 3 – The 2-D layer of **1**.

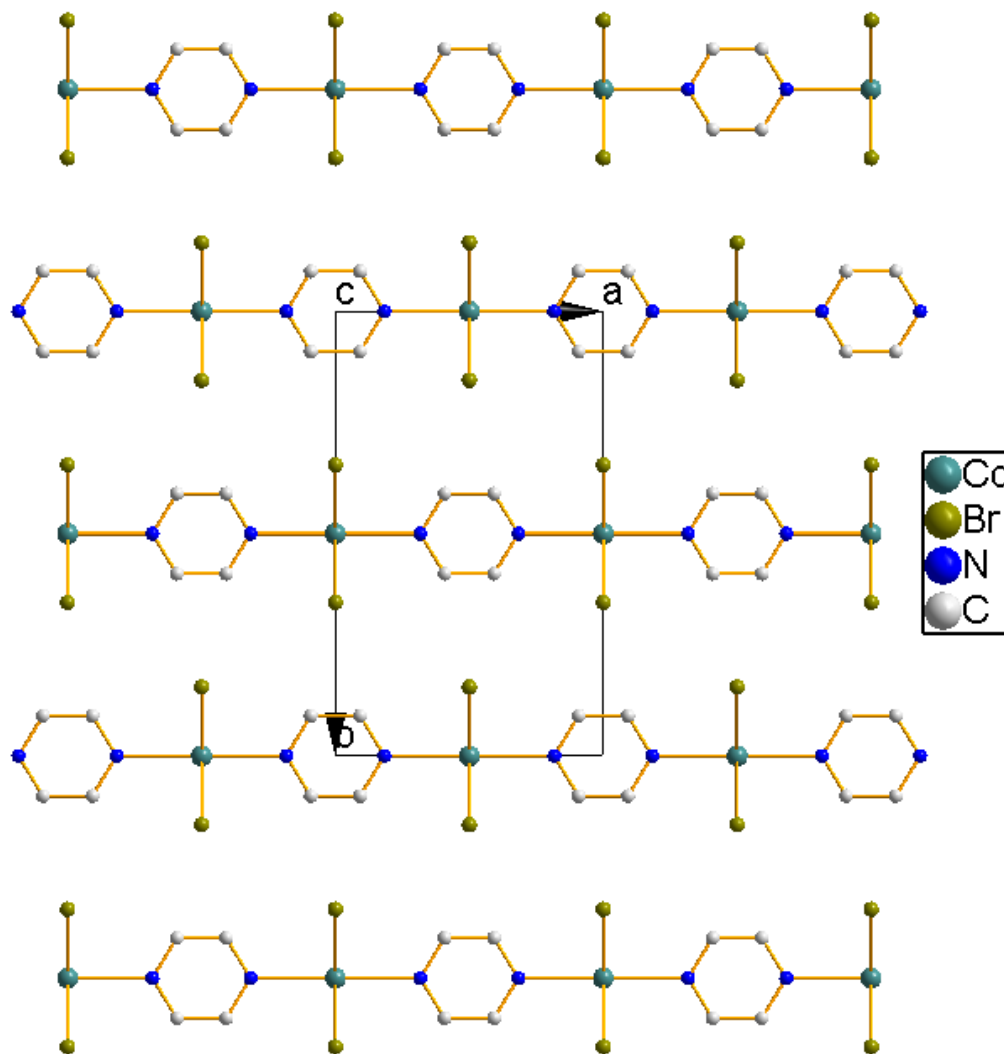


Fig. 4 – Packing diagram of 1.

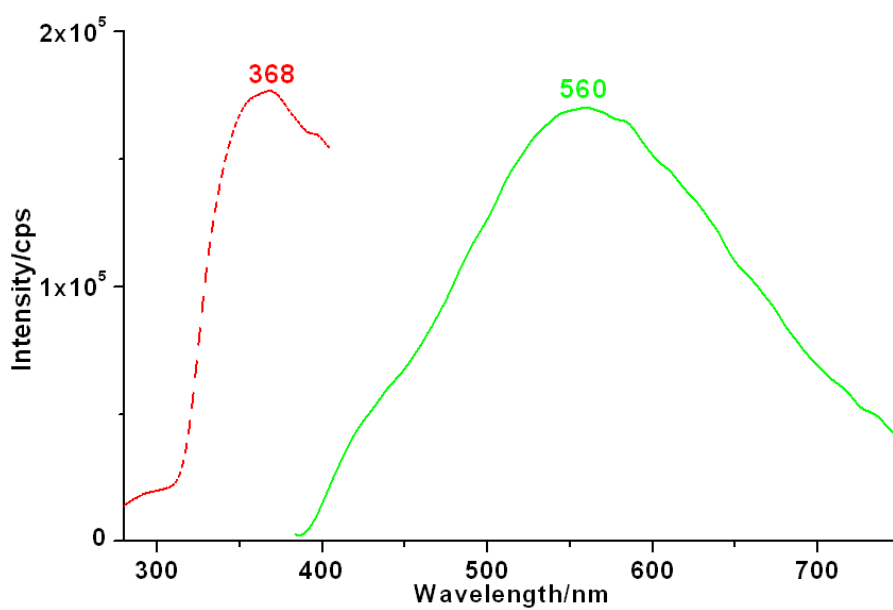


Fig. 5 – Solid-state emission and excitation spectra of 1. Solid line: emission spectra; dashed line: excitation spectra.

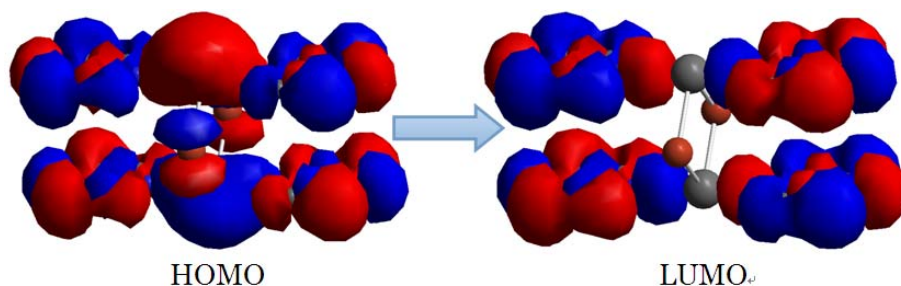


Fig. 6 – The electron-density distribution of HOMO (left) and LUMO (right) calculated for **1**. The isosurfaces correspond to electronic density differences of $-15 e \text{ nm}^{-3}$ (blue) and $+15 e \text{ nm}^{-3}$ (red).

Theoretical Calculation

For the sake of discovering the nature of the photoluminescence properties of complex **1**, we carried out the theoretical study with Gaussian03 suite of programs. In order to smoothly conducting the time-dependent DFT (TDDFT) calculation, we truncated the ground state geometry from the single-crystal X-ray diffraction data. TDDFT calculation was performed with a B3LYP function based on this ground state geometry. As depicted in Fig. 6, the result of the TDDFT study reveals the characteristics of the highest occupied molecular orbital (HOMO) and the lowest unoccupied molecular orbital (LUMO). From Fig. 6, we can clearly found that the electron density of the singlet state of the HOMO is mainly located at the cadmium and bromide ions. However, the electron density of the singlet state of the LUMO is dominantly resided in the pyrazine ligand. As a result, the theoretical study discovers that the photoluminescence emission band of **1** should be originated from the metal-to-ligand charge-transfer (MLCT) (from the HOMO of the cadmium ions to the LUMO of the pyrazine ligand) and the ligand-to-ligand charge-transfer (LLCT) (from the HOMO of the bromide ions to the LUMO of the pyrazine ligand) transitions, as displayed in Fig. 6.

CONCLUSIONS

In brief, we have successfully synthesized a novel pyrazine complex via solvothermal reactions. The title complex is characterized by single-crystal X-ray diffraction. It is characteristic of a two-dimensional layer. This complex displays a wide and intense photoluminescence emission band in the green region. Theoretical study reveals that the photoluminescence emission is originated from the metal-to-ligand charge-transfer (MLCT) and the ligand-to-ligand charge-transfer (LLCT) transition.

Acknowledgements. We gratefully acknowledge the financial support of the open foundation (ST201522007) of the Key Laboratory of Jiangxi Province for Persistent Pollutants Control and Resources Recycle (Nanchang Hangkong University), Jiangxi Provincial Department of Education's Item of Science and Technology (GJJ150761, GJJ14557, GJJ170637), the NSF of China (21361013, 21362015, 21461013), the NSF of Jiangxi Province (20133ACB20010) and the open foundation (20150019, 20180008) of the State Key Laboratory of Structural Chemistry, Fujian Institute of Research on the Structure of Matter, Chinese Academy of Sciences.

REFERENCES

1. X. Guo and C. Burda, *Coord. Chem. Rev.*, **2016**, 320–321, 53.
2. S. Taleghani, M. Mirzaei, H. Eshtiagh-Hosseini and A. Frontera, *Coord. Chem. Rev.*, **2015**, 309, 84.
3. M. Karimi, A. Badieli and G. M. Ziarani, *Inorg. Chim. Acta*, **2016**, 450, 346.
4. Q. Han, Y. Wen, J. Liu, L. Chen and J. Zhao, *Inorg. Chem. Commun.*, **2016**, 71, 54.
5. C. Bellitto, E. M. Bauer and G. Righini, *Coord. Chem. Rev.*, **2015**, 289–290, 123.
6. R. D. Costa, E. Ortí, H. J. Bolink, F. Monti, G. Accorsi and N. Armaroli, *Angew. Chem. Int. Ed.*, **2012**, 51, 8178.
7. X. J. Dui, X. Y. Wu, J. Z. Liao, T. Teng, W. M. Wu and W. B. Yang, *Inorg. Chem. Commun.*, **2016**, 56, 112.
8. M. P. Santoni, G. S. Hanan and B. Hasenknopf, *Coord. Chem. Rev.*, **2014**, 281, 64.
9. J. Guo, Y. Ping, H. Ejima, K. Alt, M. Meissner, J. J. Richardson, Y. Yan, K. Peter, D. von Elverfeldt, C. E. Hagemeyer and F. Caruso, *Angew. Chem. Int. Ed.*, **2014**, 53, 5546.
10. D. C. Hyun, N. S. Levinson, U. Jeong and Y. Xia, *Angew. Chem. Int. Ed.*, **2014**, 53, 3780.
11. D. L. Reger, J. J. Horger, M. D. Smith, G. J. Long and F. Grandjean, *Inorg. Chem.*, **2011**, 50, 686.
12. H. Y. Chen, D. R. Xiao, S. W. Yan, J. H. He, J. Yang, X. Wang, R. Yuan and E. B. Wang, *Inorg. Chim. Acta*, **2012**, 387, 283.
13. H. W. Kuai, J. Fan, Q. Liu and W. Y. Sun, *CrystEngComm*, **2012**, 14, 3708.
14. X. G. Wang, X. T. Han, Q. Zhou, Y. Wang and G. Y. Liu, *Inorg. Chim. Acta*, **2012**, 387, 460.
15. M. Zhu, J. Peng, H. J. Pang, P. P. Zhang, Y. Chen, D. D. Wang, M. G. Liu and Y. H. Wang, *J. Solid State Chem.*, **2011**, 184, 1070.

16. V. Selmani, C. P. Landee, M. M. Turnbull, J. L. Wikaira and F. Xiao, *Inorg. Chem. Commun.*, **2010**, *13*, 1399.
17. R. Cervantes, J. Tiburcio and H. Torrens, *Inorg. Chim. Acta*, **2011**, *376*, 525.
18. Q. Tang, C. J. Zhang, C. H. Zhang, H. Y. Wang, Y. G. Chen and S. X. Liu, *Inorg. Chem. Commun.*, **2012**, *15*, 238.
19. W. Chen, Z. Yao, H. Kuang, H. Chen and Z. Luo, *Synth. React. Inorg. M.*, **2015**, *45*, 952.
20. C. Jiao, Z. Sun, Y. Zhu, K. Chen, J. Zhu, C. Li, C. Wang, S. Sun, H. Tian, W. Chu, M. Zheng, W. Shao, and Y. Lu, *Inorg. Chim. Acta*, **2012**, *387*, 186.
21. H. Kuang, W. Chen, Q. Luo, Y. Xu, X. Zhang and J. Liu, *Synth. React. Inorg. M.*, **2016**, *46*, 221.
22. W. Chen. *J. Jingtangshan Univ.*, **2014**, *35*, 38.
23. F. Li, Y. Kang, Y.M. Dai and J. Zhang, *Inorg. Chem. Commun.*, **2011**, *14*, 228.
24. G.H. Eom, J.H. Kim, Y.D. Jo, E.Y. Kim, J.M. Bae, C. Kim, S.J. Kim and Y. Kim, *Inorg. Chim. Acta*, **2012**, *387*, 106.
25. W. Chen, *Synth. React. Inorg. M.*, **2015**, *45*, 315.

